

Statistical damage classification method based on wavelet packet analysis

S.S. Law^{*1}, X.Q. Zhu^{2a}, Y.J. Tian^{3b}, X.Y. Li^{4c} and S.Q. Wu^{5d}

¹Department of Civil and Environmental Engineering, Hong Kong Polytechnic University, Hung Hom, Kowloon, Hong Kong, P.R. China

²School of Computing, Engineering and Mathematics, University of Western Sydney, NSW 2751, Australia

³School of Civil Engineering, Beijing Jiaotong University, P.R. China

⁴Department of Mechanics and Civil Engineering, Jinan University, P.R. China

⁵Department of Engineering Mechanics, Southeast University, P.R. China

(Received May 13, 2011, Revised January 13, 2013, Accepted April 21, 2013)

Abstract. A novel damage classification method based on wavelet packet transform and statistical analysis is developed in this study for structural health monitoring. The response signal of a structure under an impact load is normalized and then decomposed into wavelet packet components. Energies of these wavelet packet components are then calculated to obtain the energy distribution. Statistical similarity comparison based on an F-test is used to classify the structure from changes in the wavelet packet energy distribution. A statistical indicator is developed to describe the damage extent of the structure. This approach is applied to the test results from simply supported reinforced concrete beams in the laboratory. Cases with single and two damages are created from static loading, and accelerations of the structure from under impact loads are analyzed. Results show that the method can be used with no reference baseline measurement and model for the damage monitoring and assessment of the structure with alarms at a specified significance level.

Keywords: time domain; damage; inverse problem; wavelet packet; F-test; reinforced concrete; statistics; variance; skewness; kurtosis

1. Introduction

In recent years, damage assessment of structures has drawn great attention from various engineering practitioners. Damage identification techniques can be classified into either local or global methods. Most existing techniques, such as visual, acoustics, magnetic field, eddy current etc., are effective but local in nature. They require that the vicinity of the damage is known *a priori* and the position of the structure being inspected is readily accessible. The global methods quantify the healthiness of a structure by examining changes in its vibrational characteristics or the static

*Corresponding author, Professor, E-mail: siu-seong.law@polyu.edu.hk

^aSenior Lecturer, E-mail: xinqun.zhu@uws.edu.au

^bProfessor

^cAssociate Professor

^dAssistant Professor

behaviour under load. The core of this group of methods is to seek some damage indices that are sensitive to structural damage. Doebling *et al.* (1998), Sohn *et al.* (2003), Carden and Fanning (2004) presented literature reviews on the damage assessment methodologies based on parameters such as the natural frequencies, mode shapes, mode shape curvature, flexibility matrix and stiffness matrix. However, the modal properties, such as natural frequencies and mode shapes are poor indicators of damage, and more sophisticated methods have been derived based on the second derivative of mode shapes. Also a large number of measurement locations are needed to provide sufficient resolution on the mode shapes.

Most of the vibration-based damage assessment methods require modal properties that are obtained from traditional Fourier transform (FT). However, when the damage is very small, the damage-induced changes of physical structural properties are always too insignificant to reveal the damage using the FT-based method. In addition, the measured vibration signals are often contaminated with noise. The Wavelet Transform (WT) based method for vibration signal analysis is gradually adopted in many areas due to its good time-frequency localization. Hou *et al.* (2000) used a simple structural model with multiple breakable springs subjected to harmonic excitation to show that the wavelet transform can successfully be used to identify both abrupt and cumulative damages. The wavelet packet transform (WPT) is an extension of the WT that provides complete level-by-level decomposition. The WPT enables the extraction of features from signals with combined stationary and non-stationary characteristics and arbitrary time-frequency resolution. Sun and Chang (2002) concluded that the WPT-based component energy is a sensitive condition index for structural damage assessment. This index is sensitive to changes of structural rigidity and insensitive to measurement noise. The WPT component energy combined with well-trained neural network models was used to identify the location and the severity of damage. Yam *et al.* (2003) also extracted the structural damage feature based on energy variation of structural vibration responses decomposed using wavelet packet, and neural network is used to establish the mapping between the structural damage feature and damage status. This method needs accurate model information for both the healthy and damaged conditions to train the neural network model. However, it is difficult and challenging in practice, especially for complex structures. Law *et al.* (2005) developed a method to identify damage in structures using wavelet packet sensitivity. The sensitivity of wavelet packet transform component energy with respect to local change in the system parameters is derived analytically basing on the dynamic response sensitivity. The sensitivity-based method is then used for damage detection of structures. Li and Law (2008) proposed a damage detection method based on the wavelet packet energy of covariance of measured acceleration responses of structures under ambient excitation. Ren and Sun (2008) developed a wavelet entropy based method for damage detection of structures. The relative wavelet entropy gave a measure of similarity between two probability distributions that are the wavelet energy distributions. More recently, the decentralized damage identification based on wavelet entropy indices was embedded on wireless smart sensors (Yun *et al.* 2011). The method was verified via experimental tests using a three-story shear building structure and a three-dimensional truss bridge structure. The continuous and discrete wavelet transforms were used together for damage detection with more evident damage signature than that from traditional approaches based on direct investigation with the wavelet coefficients of structural response (Gokdag 2011). Bagheri *et al.* (2011) studied the detection of linear flaws in plate structures via two-dimensional discrete wavelet transform where the local damage was modelled with arbitrary length, depth and location. Beheshti-Aval *et al.* (2011) utilized the harmonic displacement response of a damaged square plate as the input signal function in the wavelet analysis without

information on the original undamaged structure. The location of damage was identified by sudden changes in the spatial variation of the transformed response. The change in the stiffness or mass of the plate with damage will cause a localized singularity which can be identified by a wavelet analysis of the displacement response.

Because all vibration-based damage detection processes rely on experimental data with inherent uncertainties, statistical analysis procedures are necessary if one is to state in a quantifiable manner that changes in the vibration response of a structure are indicative of damage as opposed to operational and/or environmental variability (Sohn 2007). Farrar *et al.* (2001) and Sohn *et al.* (2000) cast the structural health monitoring problem in the context of a statistical pattern recognition paradigm. This paradigm can be described as a four-part process: 1) Operational evaluation; 2) data acquisition and cleansing; 3) feature extraction and data reduction; and 4) statistical model development. Most references focus on methods for extracting damage-sensitive features from vibration response measurements. Few of them take a statistical approach to quantify the observed changes in these features. Worden *et al.* (2000) developed a statistical method for damage detection using the outlier analysis. The damage sensitive features are assumed to have a Gaussian distribution with an estimated mean value and covariance matrix. The problem is one of novelty detection. Features are first extracted from a baseline system to be monitored and subsequent data are then compared to see if the new features are outliers which significantly depart from the rest of the population. In fact, many statistical procedures can be used for the problem of novelty detection and a literature review was presented by Markou and Singh (2003). Sun and Chang (2004) developed a statistical pattern classification method based on the WPT for structural health monitoring. The dominant component energies are defined as a novel condition index. Two damage indicators based on the sum of absolute difference and square sum of difference are proposed. These two indicators basically quantify the deviations of the wavelet packet signatures from the baseline reference. The statistical process control method is used to determine the threshold value for the damage indicators. Any indicator that exceeds the threshold would cause a damage alarm. Xu *et al.* (2008) presented a damage index based on the statistical moments of dynamic responses of a structure under the random excitation. The sensitivity of statistical moment to structural damage was discussed. Gul and Catbas (2009) investigated statistical pattern recognition methods in the context of structural health monitoring using two different laboratory structures. The advantages and drawbacks of the outlier analysis were discussed.

Similarity test is a simple statistical technique for novelty detection to determine whether the test sample comes from the same distribution as the reference data or not. Ruotolo and Surace (1997) using the *t*-test to detect damage in beam structures. Sohn and Farrar (2001) used the residual errors of the time series model as the damage-sensitive feature and *F*-test is used to check if the new signal has significantly changed from the closest signal selected from the reference database. Iwasaki *et al.* (2004, 2005) proposed a new automatic damage detection method using response surface methodology and statistical similarity test of the identified systems using an *F*-test. The method successfully detects the damage without the use of the modeling and learning data for the damaged structures. The response surface method was used for damage detection of structures by Fang and Perera (2009) and the significance of each parameter was evaluated through the statistical *F*-test analysis.

A structural damage can cause shifts in the vibration energy across the frequency spectrum of interest. Therefore, the energy of structural vibration response at different frequency bandwidth contains information of the structural damage, and the energy variation in one or several frequency components can indicate the damage status of the structure.

This above-mentioned property of vibration energy shifts across the frequency spectrum with damage is employed in a novel damage classification method based on wavelet packet transform and statistical analysis as shown below for structural health monitoring. The response signal of a reinforced concrete structure under an impact load is normalized and then decomposed into wavelet packet components. Energies of these wavelet packet components are then calculated, and statistical similarity test based on an F -test is used to identify damage in the reinforced concrete structures with these wavelet packet component energy distributions. A statistical indicator is developed to describe the damage extent of the structure. The validity of this approach is discussed with respect to the assumptions made for the F -statistic. Experimental study is carried out on simply supported reinforced concrete beams. Different damage cases are created using static loading. Accelerations of the structure under impact loads are analysed. Results show that the method can be used with no reference baseline measurement and model for damage monitoring and assessment of the structure with alarm for a specified significance level.

2. Wavelet packet component energy analysis

The continuous wavelet transform of a square-integrable signal $f(t)$ is defined as (Mallat 1999)

$$W_f(u, s) = f(t) \otimes \psi_s(t) = \frac{1}{\sqrt{s}} \int_{-\infty}^{+\infty} f(t) \psi^* \left(\frac{t-u}{s} \right) dt \quad (1)$$

where t is time, and \otimes denotes the convolution of two functions. $\Psi_s(t)$ is the dilation of $\Psi(t)$ by the scale factor s . u is the translation indicating the locality. $\psi^*(t)$ is the complex conjugate of $\psi(t)$ which is a mother wavelet satisfying the following admissibility condition

$$\int_{-\infty}^{+\infty} \frac{|\Psi(\omega)|^2}{|\omega|} d\omega < +\infty \quad (2)$$

where $\Psi(\omega)$ is the Fourier transform of $\psi(t)$. The existence of the integral in (2) requires that

$$\Psi(0) = 0 \quad \text{i.e.,} \quad \int_{-\infty}^{+\infty} \psi(t) dt = 0 \quad (3)$$

The reconstruction of the original signal can be expressed as

$$f(t) = \frac{1}{C_\Psi} \int_{-\infty}^{+\infty} \int_{-\infty}^{+\infty} \frac{1}{s^2} W_f(u, s) \Psi \left(\frac{t-u}{s} \right) ds du \quad (4)$$

with $C_\Psi = 2\pi \int_0^{+\infty} \left(|\Psi(r)| \right)^2 \frac{dr}{r} < \infty$.

Various forms of wavelet basis function $\psi(t)$ have been developed. One of the most useful practical methods for signal decomposition is the wavelet packet analysis. A wavelet orthonormal basis decomposes the frequency axis in dyadic intervals whose sizes have an exponential growth. Coifman *et al.* (1992) generalized this fixed dyadic construction by decomposing the frequency in intervals whose bandwidths may vary. Each frequency interval is covered by the time-frequency

boxes of wavelet packet functions that are uniformly translated in time in order to cover the whole plane.

In the present study, the vibration responses are standardized prior to wavelet transform as follow (Sohn and Farrar 2001)

$$x(t) = \frac{\hat{x}(t) - u_{\hat{x}}}{\sigma_{\hat{x}}} \tag{5}$$

where $\hat{x}(t)$ is the original signal and $u_{\hat{x}}$ and $\sigma_{\hat{x}}$ are the mean and standard deviation of $\hat{x}(t)$, respectively. The standardization procedure is applied to all measured responses. The measured response is represented by Haar wavelet basis function through the dyadic wavelet transformation. The bandwidths of each level of the dyadic wavelet transform are octaves, and this enables a direct comparison of the energy content of the wavelet packets as shown below. The WPT component function of the standardized measured response $x(t)$, i.e., $x_j^i(t)$, can be reconstructed as

$$x_j^i(t) = \sum_{k=-\infty}^{+\infty} c_{j,k}^i \psi_{j,k}^i(t) = R_j^i c_j^i = R_j^i D_j^i x(t) \tag{6}$$

where i denotes the i th WPT and j denotes the j th level of decomposition, and

$$R_j^i = [\psi_{j,0}^i \quad \psi_{j,2}^i \quad \dots \quad \psi_{j,l}^i], (l = 0, 1, \dots, N / 2^j - 1)$$

and $D_{j+1}^{2i} = H^{j+1} D_j^i$, $D_{j+1}^{2i+1} = G^{j+1} D_j^i$, $D_1^0 = H^1$, $D_1^1 = G^1$. H^{j+1} and G^{j+1} are matrices formed by the low-pass filter function and high-pass filter function respectively (Mallat 1999). c_j^i is the wavelet packet coefficients for the response with $c_j^i = D_j^i x(t)$. $\psi_{j,k}^i(t)$ is the wavelet packet function. The i th wavelet packet transform component energy of the response $x(t)$ at the j th level of decomposition, E_{xj}^i , is defined as

$$\begin{aligned} E_{xj}^i &= (x_j^i)^T (x_j^i) \\ &= x^T (R_j^i D_j^i)^T (R_j^i D_j^i) x \\ &= x^T T_j^i x \end{aligned} \tag{7}$$

A non-dimensional vector at the j th level of decomposition can be written as follows

$$P = \{p(1), p(2), \dots, p(2^{j-1})\} = \{E_{xj}^1 / E, E_{xj}^2 / E, \dots, E_{xj}^{2^{j-1}} / E\} \tag{8}$$

where $E = \sum_{i=1}^{2^{j-1}} E_{xj}^i$ is the total energy of the vibration response. $p(i)$ is the non-dimensional energy of the i th wavelet packet component. This vector is in fact the non-dimensional energy distribution in the different wavelet packets.

3. Statistical damage assessment procedure

3.1 Damage indicators based on wavelet packet analysis

The energy distribution of the response within the frequency bandwidth is represented by the different statistical moments of the distribution, and its mean, variance, skewness and kurtosis, i.e., μ , σ^2 , S and K , are taken as damage indicators in the damage classification study.

$$\begin{aligned} \mu &= \sum_{k=1}^{2^{j-1}} n_k p(n_k), \sigma^2 = \sum_{k=1}^{2^{j-1}} (n_k - \mu)^2 p(n_k) \\ S &= \frac{\sum_{k=1}^{2^{j-1}} (n_k - \mu)^3 p(n_k)}{\sigma^3}, K = \frac{\sum_{k=1}^{2^{j-1}} (n_k - \mu)^4 p(n_k)}{\sigma^4} \end{aligned} \quad (9)$$

where n_k is the number of the k th wavelet packet, and $p(n_k)$ is its probability density function.

3.2 Statistical damage assessment

We perform an analysis of variance on two groups of samples of the above damage features as

$$\mathbf{v}^0 = \{v_1^0, v_2^0, \dots, v_{N_0}^0\} \text{ and } \mathbf{v}^1 = \{v_1^1, v_2^1, \dots, v_{N_1}^1\} \quad (10)$$

where $\mathbf{v}^0, \mathbf{v}^1$ are the damage feature vectors obtained from experimental sets 0 and 1, respectively. The damage feature vector may consist of any one of the four types of damage indicators from the energy distribution of the response in Eq. (9). These indicators are random in nature and are assumed to follow the normal distribution. N_0 and N_1 are the numbers of test in experimental sets 0 and 1, respectively.

The test statistic is the F -statistic based on the F -distribution. The test is to check how large the variability is between the groups as compared to the size of the variability within each group. The assumptions behind the test are similar to the t -test in that the underlying population distribution should be normal and the population variances of the groups should be approximately equal. These two assumptions will be discussed later in this Section. In fact the F -statistic is equal to the square of the t -statistic for the analysis of variance of two groups of data (Glantz 2002), i.e., the comparison of the means of two groups in the t -test is simply a special case of analysis of variance by applying the F -statistic to the two groups. Therefore we take the experimental set 0 as the reference. The damage assessment is based on the similarity test of experimental sets 0 and 1. The null hypothesis is

$$H_0 : \mu^0 = \mu^1 \quad (11)$$

where μ^0, μ^1 are the true means of the two populations 0 and 1. The F -statistic value is defined as

$$F = \frac{MSA}{MSE} \quad (12)$$

where $MSE = \left(\sum_{k=1}^{N_0} (v_k^0 - \bar{v}^0)^2 + \sum_{k=1}^{N_1} (v_k^1 - \bar{v}^1)^2 \right) / (N_0 + N_1 - 2)$ is the between-groups variance,

$MSA = N_0 (\bar{v}^0 - \bar{\bar{v}})^2 + N_1 (\bar{v}^1 - \bar{\bar{v}})^2$ is the within-groups variance, $\bar{\bar{v}} = \frac{1}{N_0 + N_1} \left(\sum_{k=1}^{N_0} v_k^0 + \sum_{k=1}^{N_1} v_k^1 \right)$

is the overall mean of the two groups, $\bar{v}^0 = \frac{1}{N_0} \sum_{k=1}^{N_0} v_k^0$ and $\bar{v}^1 = \frac{1}{N_1} \sum_{k=1}^{N_1} v_k^1$ are the means of the two groups from population 0 and 1 respectively.

Under the null hypothesis, this F -statistic follows an F -distribution of $(p - 1, n - p)$ degrees of freedom, with $(p - 1)$ the between groups degrees of freedom and $(n - p)$ the within groups degrees of freedom, where p is the number of the groups studied and n is the total number of the data with $n = N_0 + N_1$. When the energy distributions of the responses over the frequency bandwidth from these two experimental sets exhibit similarity, the F -statistic assumes a small value. The critical value of the hypothesis H_0 is determined from a significance level α together with p and n . The critical region hypothesis H_0 is represented by the following formula

$$F > F_\alpha(p - 1, n - p) \tag{13}$$

Similarity of the features from these two experimental sets is rejected when F is larger than $F_\alpha(p - 1, n - p)$ indicating damage in the structure.

When two populations A and B are compared directly, only one F -Statistic could be obtained without a distribution. This is the disadvantage of the general homogeneity test between two populations. The statistical analysis described above is conducted as follows:

1. Ten samples were obtained separately from two populations (states) to form two DFVs as in Eq. (10). Each sample in the feature vector is obtained by the bootstrap method (Davison and Hinkley 1997) with replacement.
2. The similarity test with F -Statistic is conducted between the DFVs as in Eqs. (11) to (13).
3. Repeat Steps (1) and (2) for 200 times and 1000 times to form groups of F -statistic between two states with its own statistical distribution.

3.3 Validity of the statistical approach

The validity of the proposed approach depends on whether the population of statistical moments in Eq. (9) follow a normal distribution and the variance of the populations derived from different damage stages are approximately equal. These assumptions are justified with the proofs on the following statement on the statistical moments of the energy distribution over the frequency bandwidth calculated from the measured responses.

Statement No. 1: The response sample of a structure in each dynamic hammer test is drawn from the same population with a specific mean and variance.

Proof:

Considering a beam subjected to a hammer hitting at location x_F with an impact load denoted as $F(t)$, and the vibration response is measured at location x_s from the right end of the beam. The beam undergoes a free decay vibration with a zero initial displacement $x_{s,0}$ and an initial velocity $\dot{x}_{s,0}$ calculated as (Li and Law 2008)

$$\dot{x}_{s,0} = CF(t) \tag{14}$$

where C is a matrix of coefficient which is function of the beam mass. The dynamic response at location x_s due to the impact load can be expressed as the summation of the modal responses as

$$x_s(t) = \sum_{i=1}^m x_{si}(t) = \sum_{i=1}^m \varphi_i(x_s) \rho_i e^{-\xi_i \omega_i t} \sin(\omega_{Di} t + \theta_i) \tag{15}$$

where m is the number of mode which equals to infinity for a continuous system. $\varphi_i(x_s)$ is the value of the mode shape function at location x_s . ρ_i is the amplitude of each mode considering the initial condition. θ_i is the initial phase within $[-\pi, \pi]$. ω_i , ξ_i , ω_{Di} are the modal frequency, modal damping and natural frequency of the i th mode respectively which can be obtained as

$$\omega_{Di} = \sqrt{1 - \xi_i^2} \omega_i \tag{16}$$

$$\rho_i = \left[x_{s,0}^2 + \frac{\dot{x}_{s,0} + \xi_i \omega_i x_{s,0}}{\omega_{Di}} \right]^{1/2} \tag{17}$$

$$\theta_i = \tan^{-1} \left(\frac{\omega_{Di} x_{s,0}}{\dot{x}_{s,0} + \xi_i \omega_i x_{s,0}} \right) \tag{18}$$

Since the initial displacement $x_{s,0}$ is equal to zero, according to Eqs. (14), (17) and (18), we have

$$\rho_i = \sqrt{\frac{\dot{x}_{s,0}}{\omega_{Di}}} = \sqrt{\frac{CF(t)}{\omega_{Di}}} \tag{19}$$

and $\theta_i = 0$ or π .

According to the linear relationship between $x_s(t)$ and $x_{s,i}(t)$, the mean value of $x_s(t)$ in Eq. (15) can be expressed in terms of the mean values of $x_{s,i}(t)$

$$\mu_{xs} = E(x_s) = E(x_{s1}) + E(x_{s2}) + \dots + E(x_{sm}) \tag{20}$$

and the standard derivation of $x_s(t)$ can be expressed as

$$\begin{aligned} \sigma_{xs} &= \sqrt{Var(x_s)} = \sqrt{Var(x_{s1} + x_{s2} + \dots + x_{sm})} \\ &= \sqrt{Var(x_{s1}) + \dots + Var(x_{sm}) + \sum_{i=1}^m \sum_{j=1}^m Cov(x_{si}, x_{sj})} \quad , i \neq j \tag{21} \\ &= \sqrt{Var(x_{s1}) + \dots + Var(x_{sm}) + \sum_{i=1}^m \sum_{j=1}^m [E(x_{si} x_{sj}) - Ex_{si} Ex_{sj}]} \end{aligned}$$

It is noted that $x_s(t)$ is a response sample from one hammer hitting test and similar response samples from different hammer hitting test under the “same” testing condition after normalization may form a population with a mean and a standard deviation given by Eqs. (20) and (21), respectively.

Considering the responses at the same measured location with the “same” testing condition from two hammer tests with different amplitudes of the impact loads denoted as F_1 and F_2 , respectively. Assuming the two amplitudes have the following relationship

$$F_2 = \gamma F_1 \tag{22}$$

where γ is a constant. Since the distribution of the energy over the frequency range of interest due to the impact hammer has been guaranteed by the manufacturer of the hammer, if the response samples collected at x_s on the same structure from these two tests come from two different populations denoted as $x^{(1)}$ and $x^{(2)}$, it can be proved that the responses and their statistical moments are linearly related as

$$x_s^{(2)}(t) = \Theta x_s^{(1)}(t), \mu_{xs}^{(2)} = \Theta \mu_{xs}^{(1)}, \sigma_x^{(2)} = \Theta \sigma_x^{(1)} \tag{23}$$

where Θ is a function of γ .

According to Eq. (23) and the standardization procedure defined in Eq. (5), the response samples from two hammer tests can be finally normalized to the same x^* with zero mean and unit standard deviation as

$$\frac{x_s^{(2)} - \mu_{xs}^{(2)}}{\sigma_{xs}^{(2)}} = \frac{x_s^{(1)} - \mu_{xs}^{(1)}}{\sigma_{xs}^{(1)}} = x^* \tag{24}$$

It has been stated (Miller and Miller 2004) that, if the samples $x_s^1, x_s^2, \dots, x_s^N$ are independent and identically distributed, they will constitute a random sample from the infinite population given by their common distribution. The impact hammer tests were conducted in an independent manner, and the measured responses in each test at the same location x_s are independent to each other. The normalized response signals in Eq. (24) are shown to have the same distribution in the common population x^* . These individual samples $x_s^1, x_s^2, \dots, x_s^N$ are samples from the infinite population x^* .

Statement No. 2: The mean value μ_E of the energy spectrum over the frequency of interest obtained from impact hammer test follows a normal distribution as $N(\mu_E, \sigma_E)$.

Proof:

Statement No. 1 shows that each response from the impact hammer test has the same expression after the standardization procedure. Thus the energy of the response from each test has the same distribution over the frequency bandwidth of interest. Due to the independent way of performing each test, it can be inferred that the vector of energy distribution calculated from the wavelet transform of responses is drawn from the same population. Also we know that “even if the distribution in the original population is far from normal, the distribution of the sample means μ tends to become normal under random sampling as the size of sample increases” according to the Central Limited Theorem (Snedecor and Cochran 1989). We then draw the conclusion that the mean value of the energy spectrum from a hammer test follows a normal distribution $N(\mu_E, \sigma_E)$.

Statement No. 3: All the damage indicators in Eq. (9) follow a normal distribution.

Proof:

For the standardized response studied above, the distribution of energy follows a fixed pattern and it can be stated that the energy over a wavelet packet frequency bandwidth is linearly related

to the total energy of the standardized response. The mean value of the energy spectrum has been proved to follow a normal distribution above, and therefore the total energy of the distribution also follows a normal distribution. Because of the linear relation mentioned before, a conclusion can be inferred that the energy contained in each wavelet packet bandwidth follows a normal distribution. Since the statistical theorem (Berry and Lindgren 1996) states that “the linear combination of multiple normal distributed variables is still following a normal distribution”, we can draw the conclusion that any of the damage indicators in Eq. (9) follows a normal distribution.

The Bootstrap Method of Sampling

Traditional parametric approach to make statistical inference needs (a) to assume that the sampling distribution has a shape with known probability properties and (b) to estimate analytically the parameters of that sampling distribution. But for the present case where the energy distribution over the frequency bandwidth of the standardized response is unknown, the distributions of the statistical moments are also not available.

The bootstrap procedure is applied in this study which makes probability-based inferences about a population characteristic based on an estimator using a sample drawn from that population. The sampling technique does not require the parent population distributional assumptions and without the need for analytic formulas for the sampling distribution parameters. It empirically estimates the entire sampling distribution by examining the variation of the statistic within the sample. The basic bootstrap approach is to treat the sample as if it is the population, and apply Monte Carlo sampling to generate an empirical estimate of the statistic’s sampling distribution. This is done by randomly drawing a large number of “resamples” of size n from the original sample with unknown but identical distribution with replacement. The bootstrap approach retains the statistical characteristics of the mother structure.

Variance of the Populations

The F -statistic requires that the populations from which the samples are drawn to follow a normal distribution and the samples are independently drawn. These have been proved in the discussions above. It also requires that the variance of the populations from which the samples are drawn to be approximately equal. Another F -test on the homosecdasticity of the two groups will be conducted with the null hypothesis $H_0: \sigma_1 = \sigma_2$, where σ_1 and σ_2 are the variance of the two populations. The F -statistic is defined as $F = s_1^2 / s_2^2$ where s_1^2 is the larger group variance of the two, and s_2^2 is the smaller group variance. When the two samples come from the same population, F is equal to 1.0. The two-tailed critical region for hypothesis H_0 is represented by $F_{0.025}(n_1 - 1, n_2 - 1) > F > F_{0.0975}(n_1 - 1, n_2 - 1)$ with 5% level of significance. Hypothesis H_0 is rejected when F is outside this range.

4. Experimental setup

Two four-metre long uniform rectangular reinforced concrete beams with 3.8m simply supported span as shown in Fig. 1, were tested in the laboratory. The beam cross-section is 300mm high and 200mm wide. There are three 20mm diameter mild steel bars at the bottom of the beam, and two 6mm diameter steel bars at the top of the beam section. 6mm diameter mild steel links are provided at 195mm spacing over the whole beam length. The beam end rests on top of 50mm

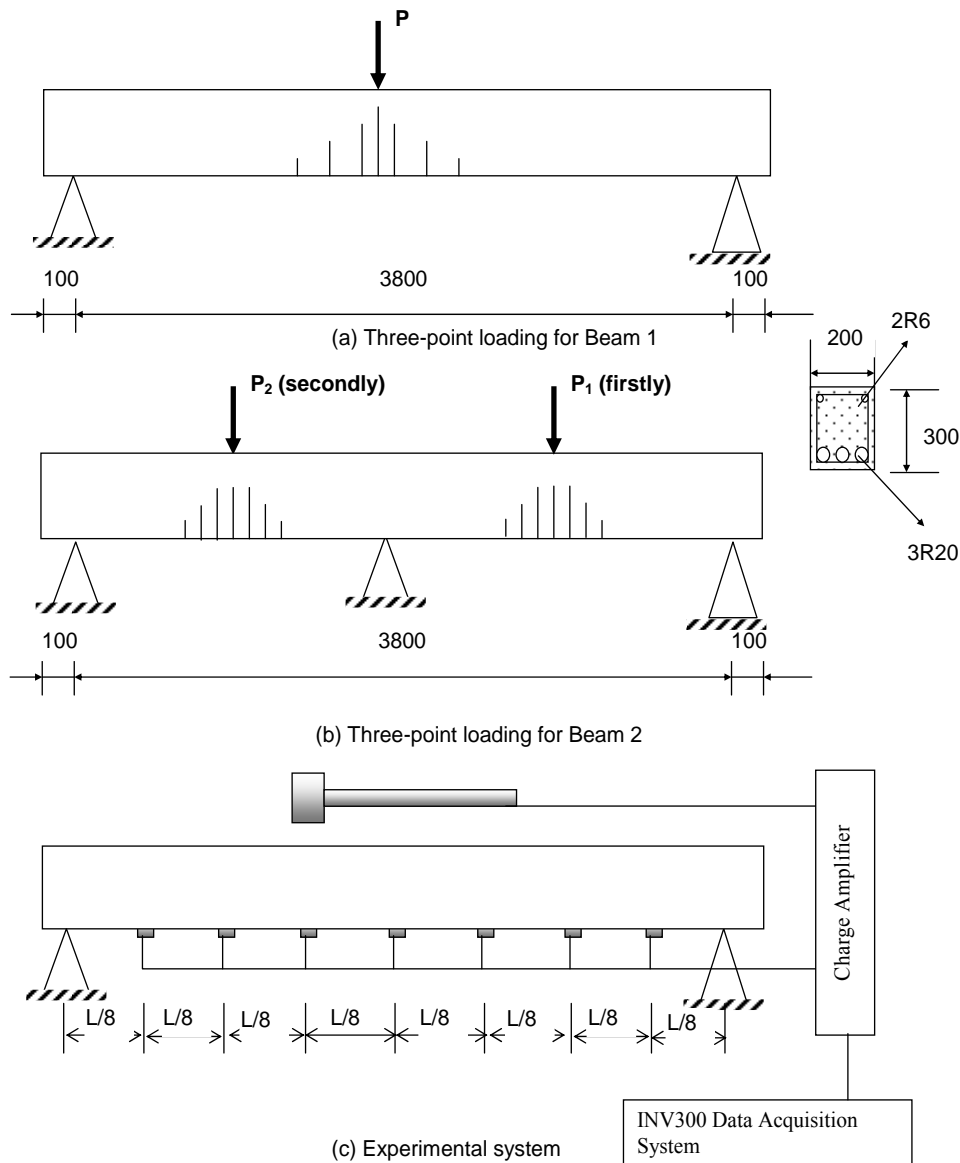


Fig. 1 Reinforced concrete beam and sensor locations

diameter steel bar at each end which in turn rests on top of a solid steel support fixed to a large concrete block on the strong floor of the laboratory. A piece of thin rubber pad is placed between the steel bar and the bottom of the concrete beam for level adjustment. The reinforcement in the two beams, namely, Beam 1 and Beam 2 corresponds to a steel percentage of 1.57%. The compression strength of concrete is 54.4MPa, and the density, tensile strength, Young's modulus, and Poisson Ratio of concrete are respectively 2351.4kg/m³, 3.77MPa, 30.2GPa and 0.16. The Young's Modulus and yield stress of the mild steel bars are respectively 181.53GPa and 300.07MPa.

Table 1 Scheme of Static load test, fundamental frequency and crack conditions

Damage States	01	02	1	2	3	4	5	6	7	8	9	10
P (kN)	0	2	10	17	25	35	45	50	55	60	67	75
Beam1 Frequency (Hz)	30.43	30.69	30.02	29.66	29.34	28.76	29.20	28.91	28.73	28.30	28.10	26.96
Beam1 Length of Crack Zone (m)	0.00	0.00	-	-	1.213	1.801	1.801	-	-	-	2.399	2.399
Beam1 Max. height of crack (mm)	0.00	0.00	-	92 (1)	132 (7)	166(11)	181(11)	-	-	-	192(14)	300(14)
P (kN)	0	-	20 (R)	50 (R)	80 (R)	110 (R)	20 (L)	50 (L)	80 (L)	110 (L)	150 (L)	150 (R)
Beam2 Frequency (Hz)	32.61	-	32.57	32.11	31.98	31.87	31.41	30.64	30.77	30.90	30.04	29.67
Beam2 Length of Crack Zone (m)	0.00	-	-	0.309	0.798	0.998	-	0.415	1.038	1.165	1.165	0.998
Beam2 Max. height of crack (mm)	0.00	-	-	113 (2)	134 (6)	164 (7)	-	124 (3)	144 (6)	173 (8)	200 (9)	240 (8)

Note: 1) *R* denotes loading location at $3/4L$; 2) *L* denotes loading location at $1/4L$; 3) Others at $1/2L$; 4) (●) denotes number of cracks; 5) –denotes no measurement is recorded.

5. Damage detection of beams with single damage zone

5.1 Test procedure

Beam 1 was incrementally loaded at mid-span to different static load levels creating a single damage zone using three-point loading as shown in Fig. 1(a). The load levels were from zero up to the failure load of the beam. The crack locations and lengths were monitored in addition to the displacement measurements. Details of the loading steps and the crack damage conditions are listed in Table 1. At each load level, twenty impact hammer tests were conducted after the beam had been unloaded for twenty minutes. Seven accelerometers evenly distributed at the bottom and along the beam as shown in Fig. 1(c) measured the responses. Impact force excitation was applied at $3/8L$ from the left support using a Dytran Instruments model 5803A 12 lbs instrumented impulse hammer. INV300 data acquisition system was used to collect the data from all the 8 channels. Sampling frequency is 2000Hz, and 8192 data were recorded for each hammer test. The fundamental frequency of the beam at each load level is also shown in Table 1. The fundamental frequency is noted to reduce with increase of damage at each load level.

5.2 Analysis on the damage indicators

The first 1000 data of the response from $5/8L$ were decomposed into six levels of wavelet packets. The frequency bandwidth of each decomposed wavelet packet is 15.625Hz. Fig. 2 shows the measured responses, their Fourier spectrum and wavelet packet components at $5/8L$ for different damage states. Only the first 32 WP are shown in the figure because the remaining WP contains very small vibration energy. Table 2 shows the average values of the four damage indicators from Eq. (9) for all states. Fig. 3 shows the range and average of the damage indicator (mean) for all states. Fig. 4 shows the average damage indicator (mean) for all states from different measuring locations. The following observations are obtained from these results:

Table 2 Average damage indicators for Beam1 from responses at 5/8L

Damage States	01	02	1	2	3	4	5	6	7	8	9	10
Mean	7.65	7.43	5.86	6.16	5.76	4.50	5.32	5.38	5.47	4.56	4.25	5.11
Variance	9.44	9.23	6.54	7.28	6.80	4.72	6.00	5.99	6.08	4.94	4.34	6.08
Skewness	3.09	3.15	3.93	3.82	4.08	5.33	4.55	4.15	4.09	4.67	4.87	4.58
Kurtosis	14.01	14.28	23.07	21.54	24.80	44.25	31.27	27.18	26.25	34.64	38.71	32.37

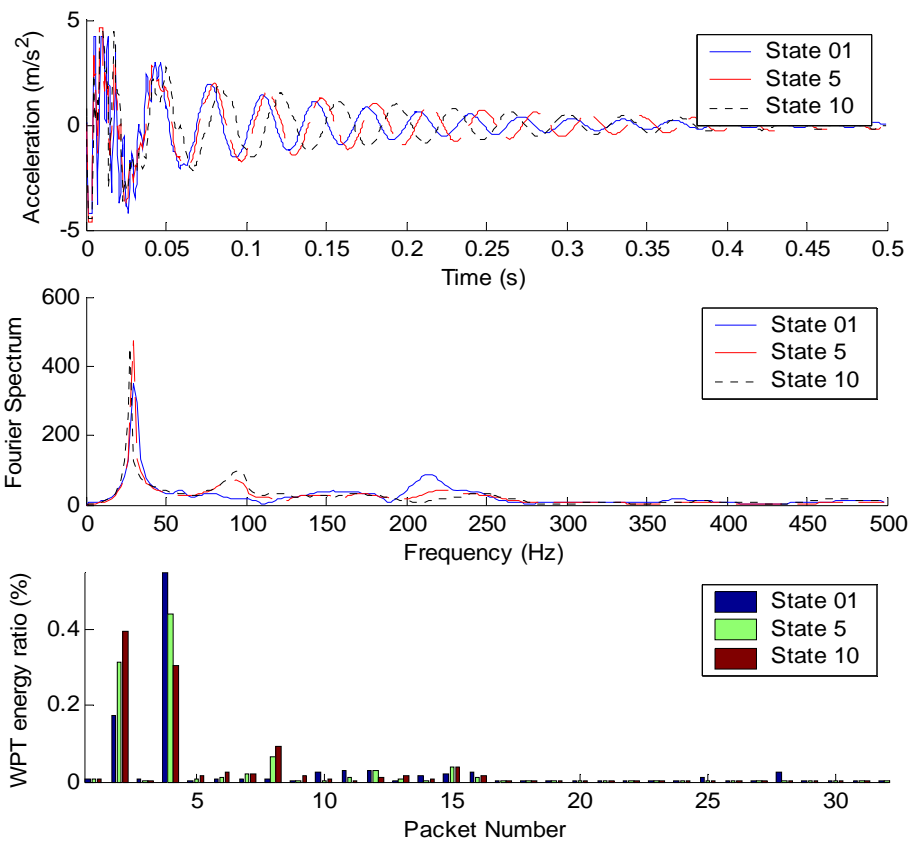


Fig. 2 Impact responses and their spectrum at 5/8L for Beam 1

1) The wavelet packet component energy changes with the different damage states as shown in Fig. 2. The energy ratio of the second wavelet packet component increases with the damage state number while that in the fourth component reduces. This shows that the energy change of the wavelet packet components is clearly related with damage in the reinforced concrete beam.

2) Observations in Fig. 3 and Table 2 show that all the states can be classified into six groups according to their damage indicator (mean): States 01 and 02 form the first group. States 1, 2 and 3 are in the second group. State 4 is the third group. States 5, 6 and 7 form the fourth group. States 8 and 9 are in the fifth group and State 10 is the sixth group. The average values of the damage

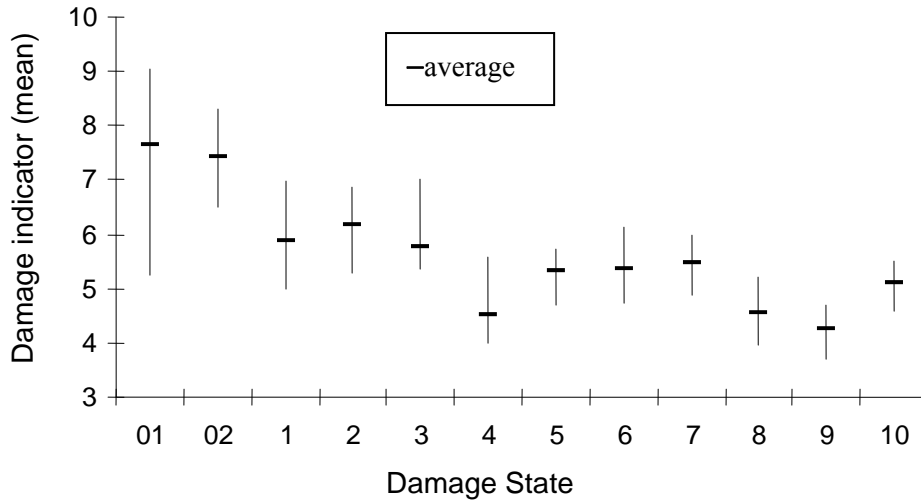


Fig. 3 Damage indicator (mean) at $5/8L$ of all states for Beam 1

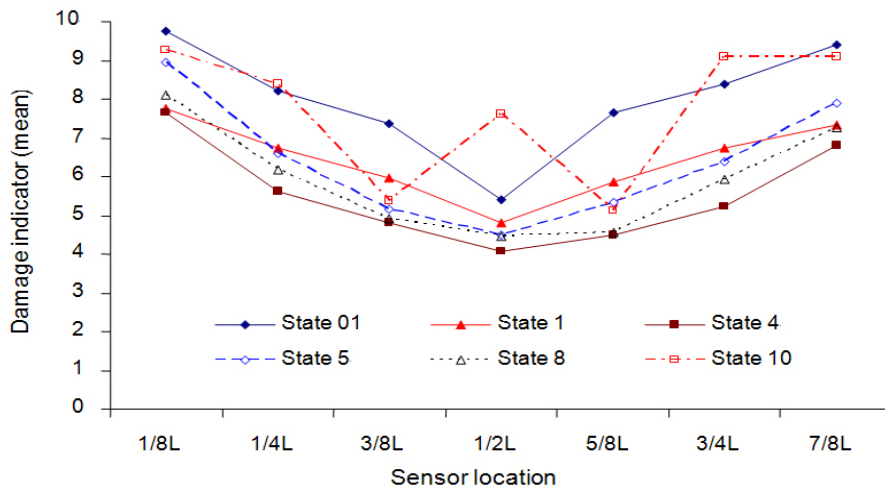


Fig. 4 Damage indicator (mean) from responses at different measuring locations

indicators are close to each other in each group. The fundamental frequency in Table 1 also show similar pattern. Therefore the damage process of Beam 1 can be represented by these groups, which are renamed as six configurations with distinctly different behaviour and damage pattern. The average variance, skewness and kurtosis in Table 2 also exhibit similar pattern as the average mean.

3) Fig. 4 shows that the average damage indicator (mean) is different at different measuring locations. Since the damage in beam is symmetrical about mid-span, the indicators at $1/8L$ and $7/8L$, $1/4L$ and $3/4L$, $3/8L$ and $5/8L$ are close to each other and are in pairs. It is noted that this damage indicator is a measure of the central frequency of the energy distribution in the frequency spectrum. Different measured location corresponds to a different combination of the modal responses. Fig. 4 shows that the first five configurations exhibit similar behaviour throughout the

damage process, while the final damage configuration which corresponds to a failure state, has significantly different composition of response components as measured at mid-span. This means that any sensor could give an indication of the damage process as seen in Fig. 4 but sensor when located at the damage could detect drastic change in the indicator associated with failure of the cross-section.

5.3 Similarity test of wavelet packet energy ratios using *F*-test

The probability distribution of the *F*-statistical value in a similarity test for two sets of data follows $F(p-1, n-p)$ distribution if they come from the same state. In this study, $p = 2$ and $n = 20$, and the probability distribution of the *F*-statistical value may follow $F(1, 18)$ distribution. Two significance levels α for the *F*-similarity test are selected as 1% and 5% corresponding to critical values of $F_1 = F_{0.05}(1, 18) = 4.41$ and $F_2 = F_{0.01}(1, 18) = 8.29$. When *F* exceeds one of these values, similarity between groups of data from two different states is rejected. If one state is the intact state, the structure is diagnosed as being damaged.

Feature vectors \mathbf{v}^0 and \mathbf{v}^1 are formed from the twenty test results for each state with ten randomly selected components each, and the *F*-statistical value is calculated by Eq. (12). 200 different combinations of the test results are used in the calculation. (The use of 1000 combinations of test results has been checked yielding similar results). Fig. 5 shows the distribution of the experimental *F*-statistical values for the undamaged case from responses at $5/8L$ and the $F(1, 18)$ distribution. Both sets of data for comparison are taken from the intact specimen.

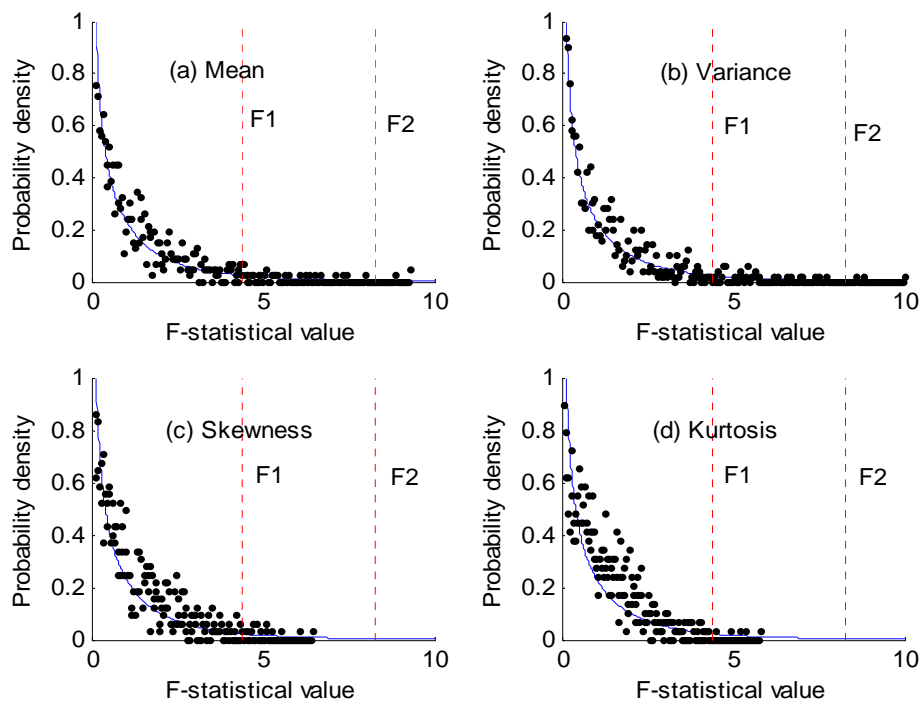


Fig. 5 Distribution of *F*-statistical values for different damage indicators for the intact beam (— $F(1, 18)$ distribution, ... *F*-statistical values (mean))

Table 3 The average F -statistical values of the damage indicators from responses at $5/8L$ (Beam 1)

Damage States	01	02	1	2	3	4	5	6	7	8	9	10	
Mean	$i \sim i$	1.00	1.07	1.19	1.11	1.15	1.12	1.03	1.17	1.09	1.19	1.11	1.05
	$i \sim 0$	-	1.44	42.12	32.18	51.32	152.46	87.32	83.48	75.05	150.77	179.35	106.26
	$i \sim i-1$	-	1.49	49.75	3.44	7.56	69.51	44.26	0.70	1.40	54.88	7.22	58.34
Variance	$i \sim i$	1.00	1.07	1.17	1.10	1.15	1.11	1.00	1.23	1.08	1.20	1.10	1.03
	$i \sim 0$	-	1.16	39.64	22.48	31.36	95.75	56.98	53.95	54.38	90.30	104.70	60.09
	$i \sim i-1$	-	1.20	50.83	4.96	2.98	33.64	19.16	0.60	0.75	17.61	7.40	64.39
Skewness	$i \sim i$	1.00	1.05	1.08	1.18	1.07	1.15	1.10	1.16	1.16	1.11	1.08	1.04
	$i \sim 0$	-	1.09	22.92	38.48	61.12	115.58	113.26	75.36	74.15	69.00	63.35	141.78
	$i \sim i-1$	-	1.13	23.20	1.11	9.97	44.32	18.15	16.23	0.97	17.92	1.23	2.27
Kurtosis	$i \sim i$	1.00	1.04	1.13	1.07	1.18	1.09	1.08	1.09	1.18	1.08	1.06	1.02
	$i \sim 0$	-	1.01	23.22	35.42	60.81	106.65	96.71	113.83	123.34	63.78	52.70	208.07
	$i \sim i-1$	-	1.06	25.85	1.14	8.36	45.84	20.01	9.28	1.48	18.03	1.46	3.35

Note: 0 denotes the intact State 01; i denotes the i th damage state

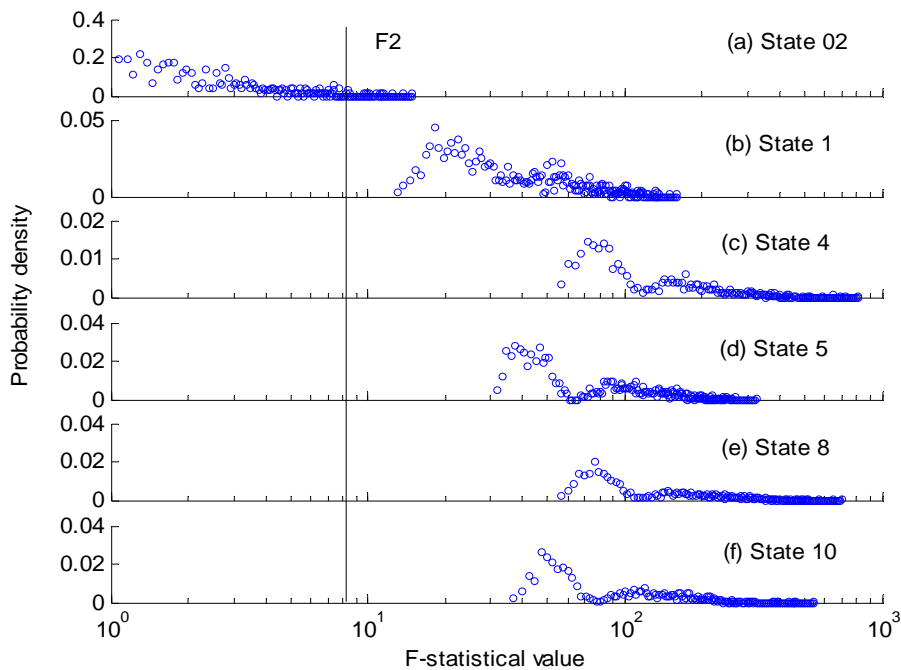


Fig. 6 Distribution of F -statistical values (mean) for Beam 1 (State i versus State 01)

The vertical dash lines show the critical values at the significance levels 1% and 5%, respectively. Table 3 shows the average F -statistical values for the four damage indicators from the responses at $5/8L$. Fig. 6 shows the distribution of F -statistical values (mean) for different configurations of the reinforced concrete beam compared to the intact State 01. Fig. 7 shows the

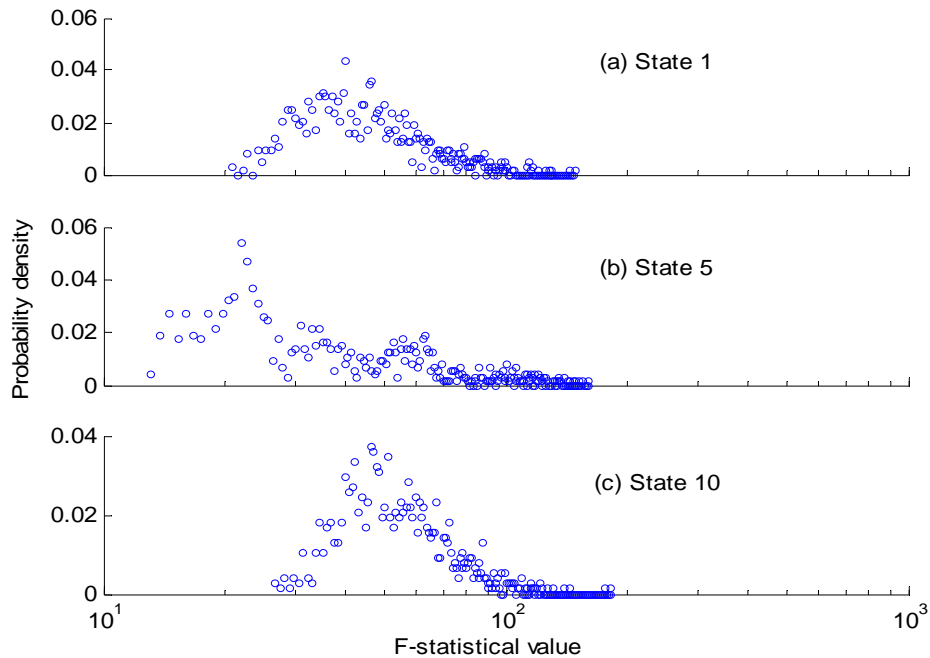


Fig. 7 Distribution of F -statistical values (mean) for Beam 1 (State i versus State $i-1$)

distribution of F -statistical values (mean) from comparison between two successive states. The following observations are obtained from these results:

1) The distribution of the F -statistical values for the four damage indicators in Fig. 5 is close to the theoretical $F(1,18)$ distribution. This comparison confirms the feasibility of the F -test in the acceptance of the null hypothesis with a specified significance level when comparison is made within the intact state.

2) From Table 3, the average of the F -statistical value (mean) is close to 1.0 when the similarity test is performed on data from the same state. Fig. 6 shows that the probability for the F -statistical value for State 02 which is larger than the critical value F_2 is very small. The critical values F_1 and F_2 may be taken as the threshold of acceptance for the null hypothesis. The average F -statistical value (mean) for States 1 to 10 compared with State 01 are all larger than F_2 as shown in Table 3 and Fig. 6. This indicates that there is an obvious change from the initial state. The F -statistical value increases basically with the damage state number, except for State 4 which has a high surge in the values. These results show that the F -statistical value could be used as an indicator of the damage state.

3) The F -statistical values from two adjacent states are also shown in Table 3. The values are large for State 1 versus State 0, 4 versus 3, 5 versus 4, 8 versus 7 and 10 versus 9 indicating large changes between these two states. This confirms observation in Table 2 and Fig. 4 leading to the grouping of the different damage states into six damage configurations. The F -statistical value of two adjacent states is an effective indicator for structural health monitoring when the baseline information is not available. Fig. 7 shows the distribution of the F -statistical values for States 1 versus 0, 5 versus 4 and 10 versus 9. The distributions are very close to each other. It shows the

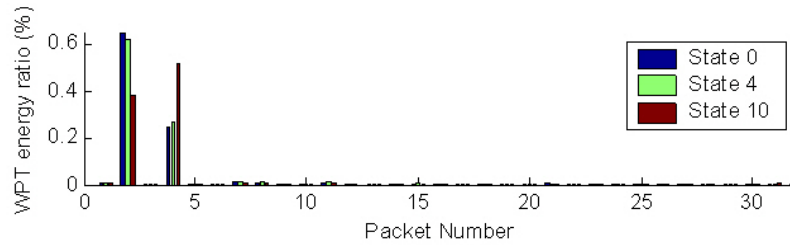


Fig. 8 Wavelet packet energy ratio at 1/2L for beam 2

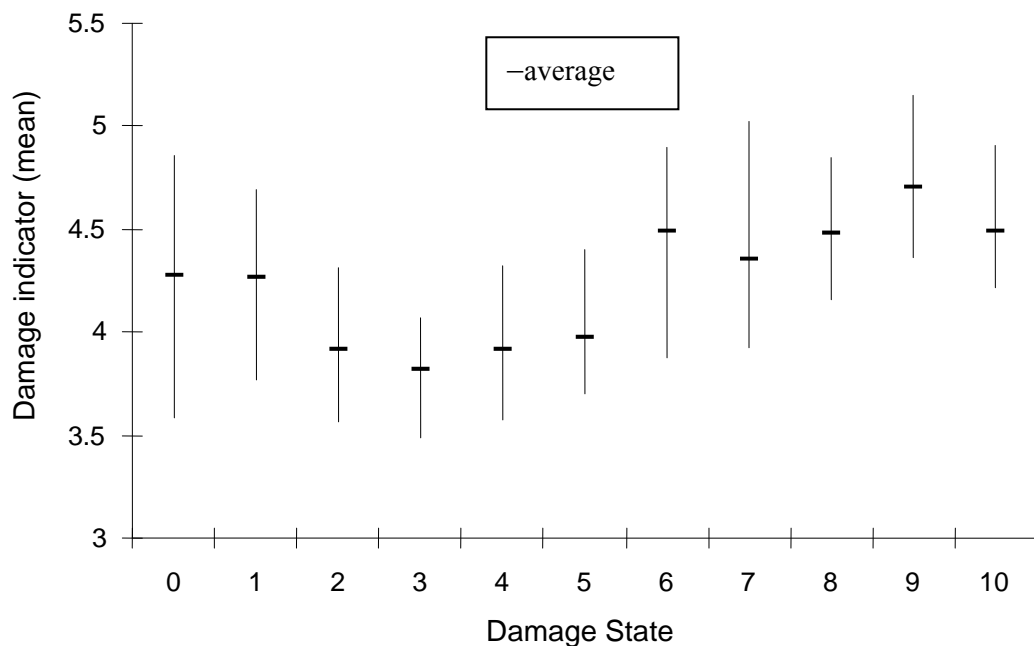


Fig. 9 Damage indicator (mean) at 1/2L of all states for Beam 2

relative changes between two adjacent states in the three sets of comparison are similar.

It is noted that the measurement location governs the basic energy distribution of the response. The damage pattern in Beam 1 is basically at mid-span affecting mainly the fundamental mode with little changes for the second and higher modes. Measurement from 5/8L basically picks up all these changes. Another study with Beam 2 is made below with the damage not at mid-span but with the measurement from mid-span to check on the performance of the different damage indicators for a comparison.

6. Damage detection of two damage zones

6.1 Test procedure

The experimental set-up is the same as above. Beam 2 was also incrementally loaded but firstly

at $3/4L$ and then at $1/4L$ position as shown in Table 1. An extra support was placed in the middle of the beam for both loading positions to create two zones of crack damages as shown in Fig. 1(b). Details of the loading steps and the crack conditions are listed in Table 1. At each load level, twenty impact hammer tests were conducted after the beam was unloaded for twenty minutes and with the support at mid-span removed. The fundamental frequency of the beams at each load level is also shown in Table 1. The frequency again reduces with increasing damage as in Beam 1.

6.2 Similarity test of wavelet packet energy ratios using F -test

Similar to the study for Beam 1, 200 different damage feature vectors, each with ten components, formed from the twenty impact tests were analysed. Fig. 8 shows the wavelet packet component energy from responses at $1/2L$. Fig. 9 shows the range and the average damage indicators of all damage states for Beam 2. Fig. 10 shows the F -statistical values (mean) compared to the intact state. Table 4 shows the averages of the four damage indicators. Fig. 11 shows the distribution of the F -statistical values (mean) from comparison between two adjacent states. The following observations are obtained from these results:

1) The energy ratio in Fig. 8 exhibit a different shift of energy in the frequency spectrum compared with that in Beam 1. The second wavelet packet component reduces with damage while those in the fourth component increases. This corresponds to a shift of vibration energy from the fundamental mode to the second and higher modes associated with the damages at quarter-span.

2) The damage indicator (mean) in Fig. 9 has a sudden drop in State 2 and a sudden jump in State 6. It has a gradual increase from States 2 to 5 and from States 7 to 9. This observation is slightly different in the higher order statistics as given in Table 4 indicating different behaviours of the four damage indicators.

3) According to the damage indicators in Tables 4 and 5 and Fig. 9, the damage states can also be grouped into four damage configurations. States 0 and 1, States 2 to 5, States 6 to 9, and State 10 correspond to the four configurations in sequence. The damage indicators are close to each other in each configuration, and the F -statistical values from two adjacent states are smaller than the critical value at significance level of 1%. These indicate that there is no obvious difference between two adjacent states in each configuration.

4) The distributions of the F -statistical values for the small damage State 1 is close to the $F(1,18)$ distribution as shown in Fig. 10(a), and the probability for $F > F_1$ is very small. There is strong indication of local damage in States 2 and 3 with most of the F -statistical values larger than F_1 . But this indication decreases with a gradual growth of the crack zone from 0.309m to 0.998m in State 2 to State 4. Further loading at $1/4L$ in States 5 and 6 erodes this indication still further until State 7 where the energy distribution of the response is similar to a uniform beam. This can be explained that a longer crack zone at mid-span has little effect on the higher modes while an

Table 4 Average damage indicators for Beam 2 from responses at $1/2L$

Damage States	0	1	2	3	4	5	6	7	8	9	10
Mean	4.27	4.27	3.91	3.81	3.91	3.97	4.49	4.35	4.48	4.71	4.49
Variance	6.8	6.72	5.82	5.62	5.5	5.61	5.36	5.27	5.25	5.81	5.82
Skewness	4.72	4.78	5.57	5.7	5.65	5.93	5.96	6.07	5.69	5.01	5.34
Kurtosis	29.6	30.28	42.71	44.41	44.17	47.25	47.95	49.64	44.21	34.15	38.3

Table 5 The average F -statistical values of the damage indicators from responses at $1/2L$ (Beam 2)

Damage States		0	1	2	3	4	5	6	7	8	9	10
Mean	$i \sim i$	1.00	1.06	1.06	1.05	1.11	1.13	1.17	1.19	1.02	1.14	1.15
	$i \sim 0$	-	0.74	8.92	19.51	8.99	6.86	3.08	0.97	3.55	12.21	3.88
	$i \sim i-1$	-	0.73	13.38	2.14	2.15	1.08	21.93	2.15	2.48	6.03	5.88
Variance	$i \sim i$	1.00	1.05	1.06	1.04	1.11	1.16	1.14	1.19	1.11	1.13	1.16
	$i \sim 0$	-	0.82	8.53	17.8	17.9	14.66	18.4	19.94	24.91	11.31	12.43
	$i \sim i-1$	-	0.82	9.86	1.51	1.25	0.83	1.36	0.76	0.72	6.04	0.47
Skewness	$i \sim i$	1.00	1.11	1.11	1.04	1.07	1.15	1.14	1.21	1.24	1.02	1.19
	$i \sim 0$	-	0.99	18.17	32.2	29.19	30.9	34.95	36.36	22.45	5.07	16.42
	$i \sim i-1$	-	0.98	25.44	1.53	1.13	4.32	0.61	0.85	4.29	24.71	16.59
Kurtosis	$i \sim i$	1.00	1.1	1.1	1.03	1.07	1.16	1.16	1.21	1.22	1.03	1.17
	$i \sim 0$	-	0.96	17.66	33.4	30.71	29.6	29.01	31.39	26.67	6.92	17.63
	$i \sim i-1$	-	0.95	22.48	1.21	0.97	2.26	0.67	0.78	3.55	25.94	11.85

Note: 0 denotes the intact State 01; i denotes the i th damage state

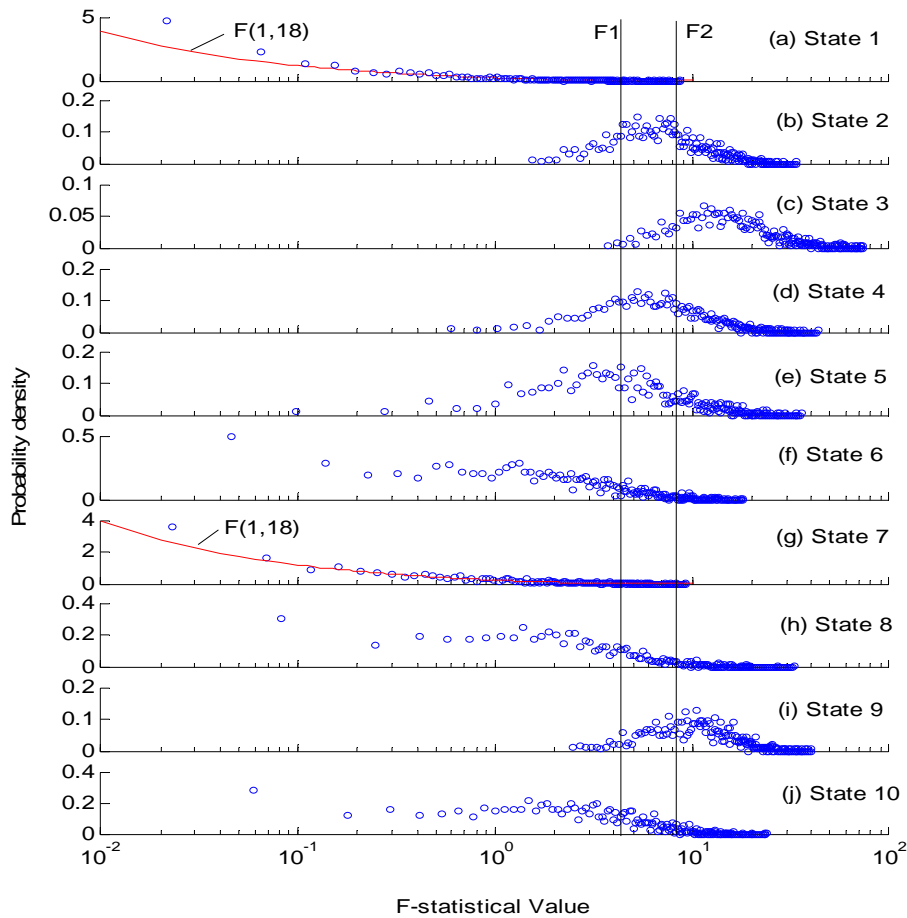


Fig. 10 Distribution of F -statistical values (mean) for Beam 2 (State i versus State 0)

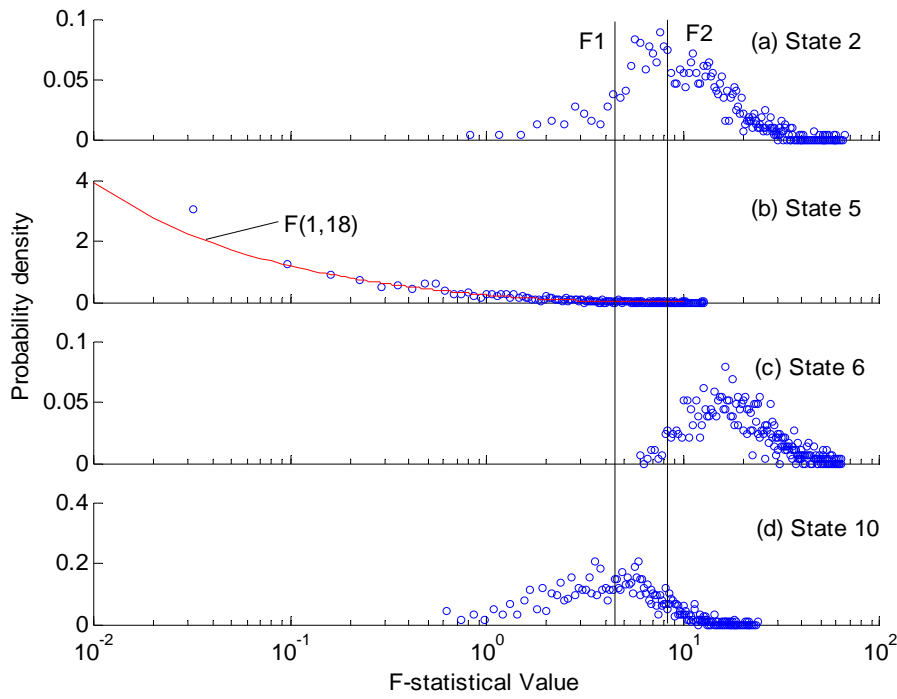


Fig. 11 Distribution of F -statistical values (mean) for Beam 2 (State i versus State $i-1$)

additional damage at $1/4L$ would remove some of the effect of unsymmetrical damage on the vibration mode shape. The two almost equal crack zones in State 7 gives rise to a symmetrical fundamental mode shape, and the composition of the response at mid-span is very similar to that of the intact beam. Further loading at $1/4L$ gives rise to the next unsymmetrical damage pattern which can be identified in Figs. 10(h) and 10(i). The final symmetrical damage State 10 has the vibration mode shapes similar to those of an intact beam.

5) Fig. 11 indicates that there is distinct difference between two adjacent States of State 2 with State 1, State 6 with State 5 and State 10 with State 9 with most of the F -statistical values larger than F_1 . This observation supports the grouping of damage configurations as discussed in Item 3 above.

It may be concluded that the F -statistical value (mean) from $5/8L$ can be used to monitor the development of unsymmetrical local damages but it is not sensitive enough to raise alarm with most of the F -statistical values smaller than F_1 . This is because the change in the higher frequencies due to the damage is small and has little effect on the energy distribution. The F -statistical values of higher order statistics are further calculated to check on their performances in the damage detection.

6.3 F -statistical values of the higher order statistics

The F -statistical value is computed for the higher order statistics of the WP component energy distribution for both beams. Sets of data from each state are compared with the intact state. The

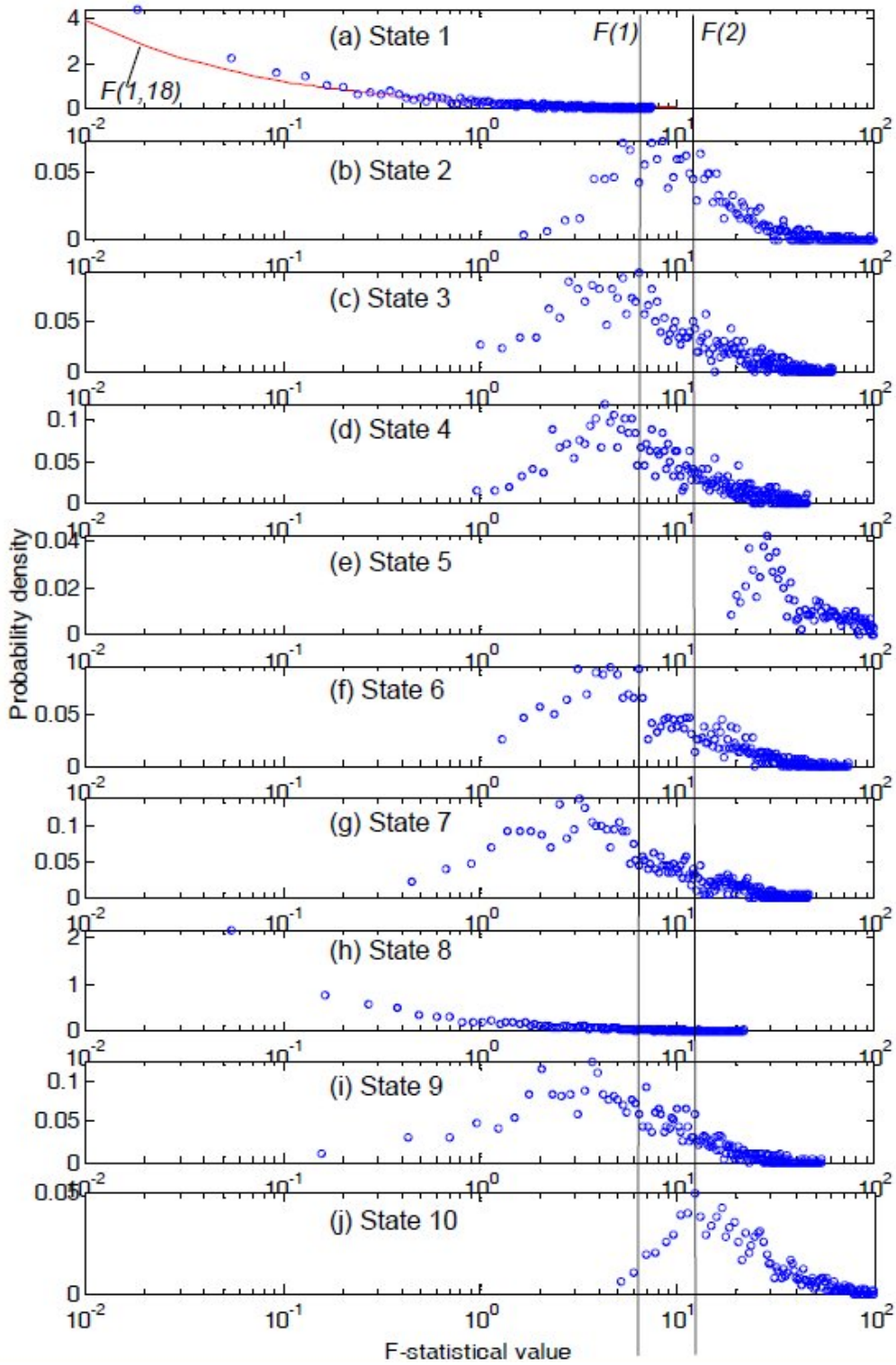


Fig. 12 Distribution of F -statistical values (variance) for Beam 1 (State i versus State 01)

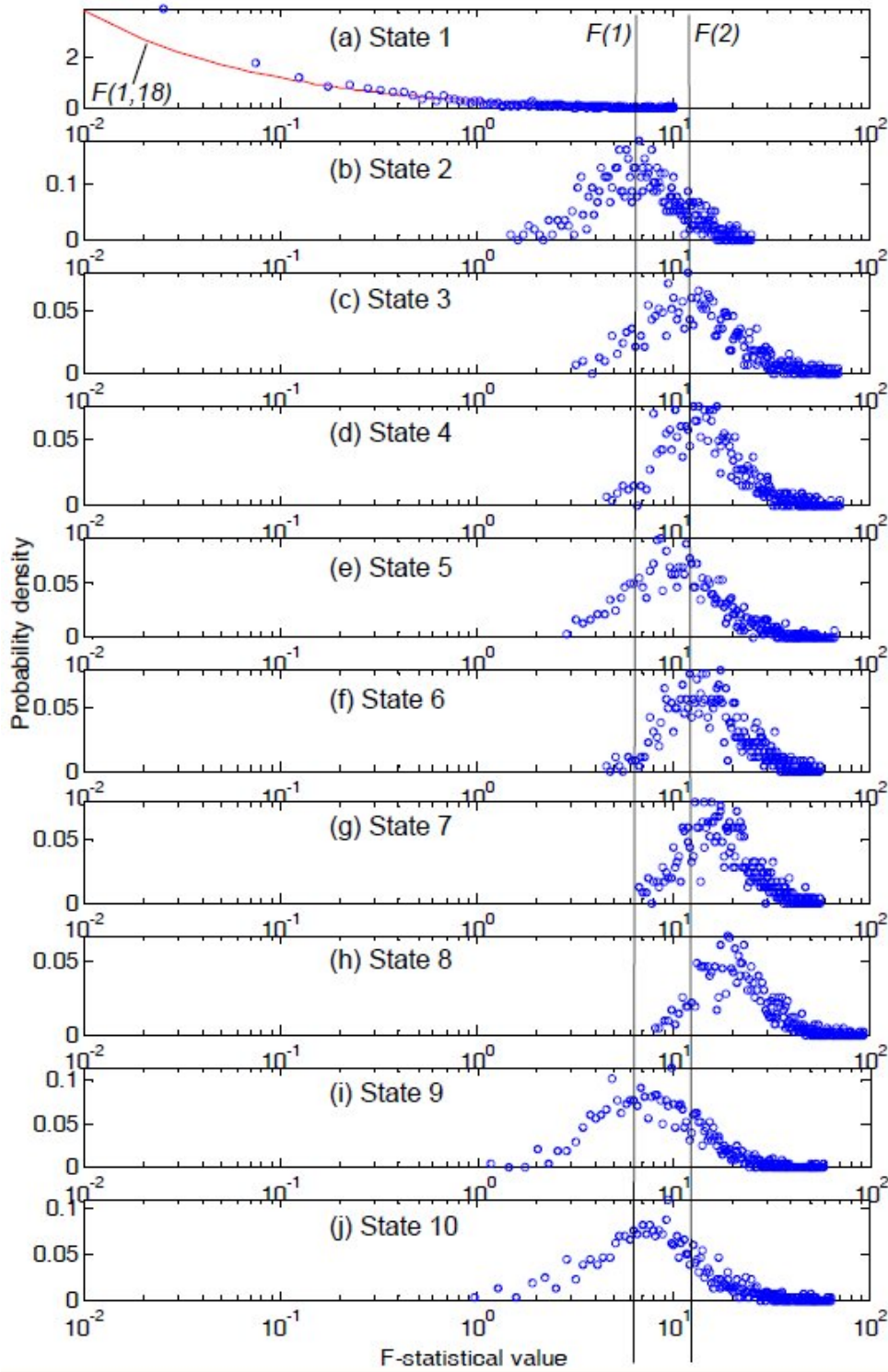


Fig. 13 Distribution of F -statistical values (variance) for Beam 2 (State i versus State 01)

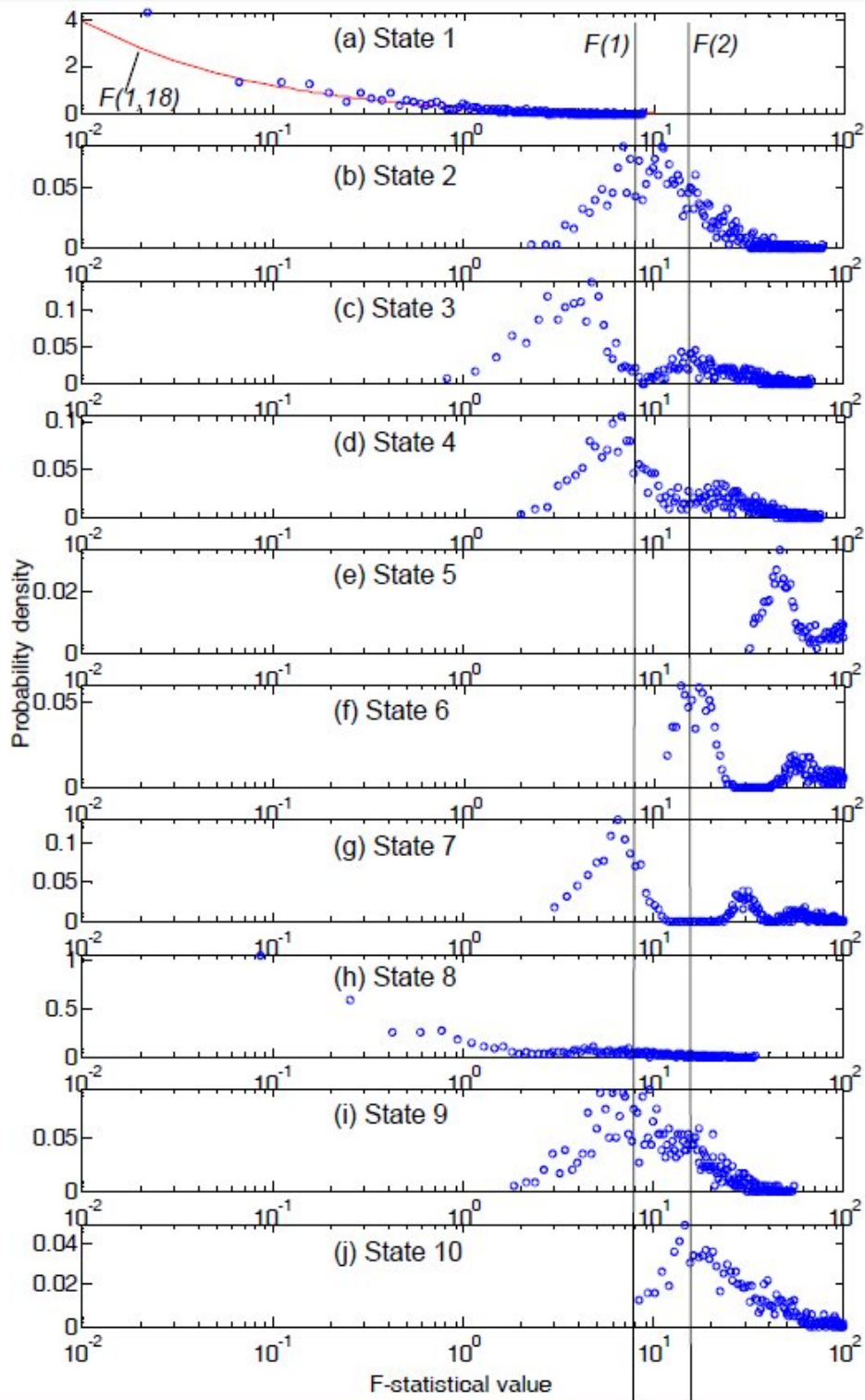


Fig. 14 Distribution of F -statistical values (skewness) for Beam 1 (State i versus State 01)

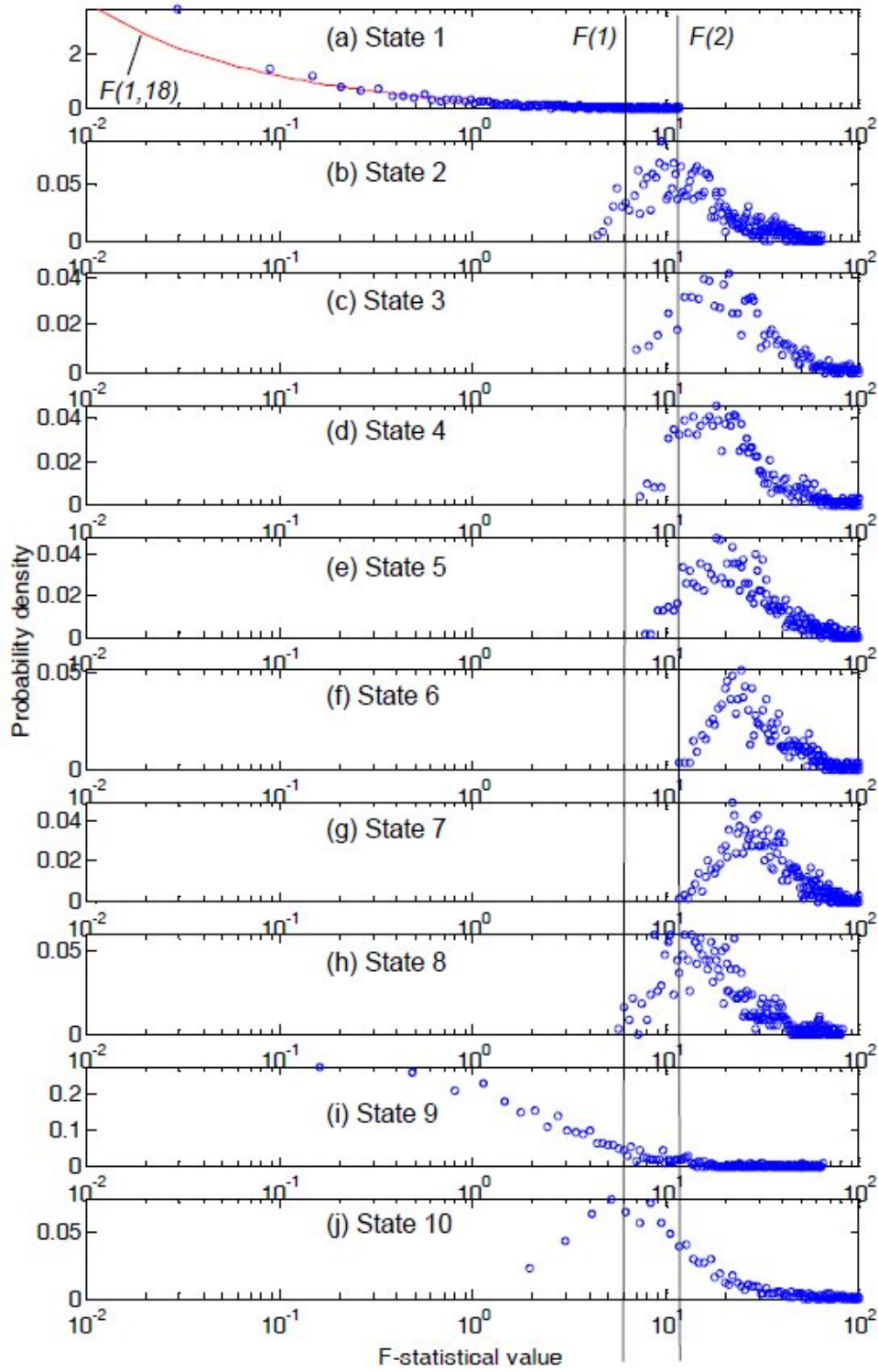


Fig. 15 Distribution of F -statistical values (skewness) for Beam 2 (State i versus State 01)

distributions of the F -statistical value of the variance for Beams 1 and 2 are shown in Figs. 12 and 13, while those for the skewness and kurtosis for each beam are very similar, and the distribution of the former for each damage state is shown in Figs. 14 and 15 for Beams 1 and 2 respectively.

The distribution of variance for both beams show the same trend of changes with damage with most the F -statistical values larger than F_1 in States 1 to 10. State 8 for Beam 1 however, exhibits a distribution closer to but not exactly the same as that of an intact beam. This can be explained considering the flexural stiffness value of a cracked section. When a concrete section is cracked seriously, the flexural stiffness of the section does not change much with further loading with a small change in the neutral axis (Law *et al.* 1995). A long seriously cracked zone would mean a zone with approximately equal flexural stiffness leading to the behaviour of a close-to-intact beam. The variance is a good indicator of damage close to mid-span.

Comparison of Figs. 6 and 14 as well as Figs. 10 and 15 indicates that the skewness is superior to the mean in all States with most of the F -statistical values larger than F_1 except in the case of very small damage in State 2. The final damage State 8 in Beam 1 and State 9 in Beam 2, however, exhibit a distribution closer to but not exactly the same as that of an intact beam. The explanation is similar to that for State 8 in Beam 1 for the variance distribution with a long and extensive cracked zone at mid-span of the beam.

It may be concluded that with the measurement from mid-span, the mean is not sensitive to local damages affecting the higher modes, while the skewness and kurtosis are more robust to detect local damages at different locations of the structure. The damage from a long and extensive cracked zone in the span may be difficult to identify, but such type of damage would be easily noted by visual inspection. The present tool can serve as a magnifying glass in the case with a large structure with many structural components. Selected ranges of WP component energy can be analysis and monitored which have been studied to associate with damage in certain critical member of the structure which is desirable to monitor throughout their life time.

7. Conclusions

A novel methodology for structural health monitoring has been developed based on statistical similarity using an F -test. A statistical indicator based on F -statistical value is presented to describe the damage extent of the structure. Experimental results in the laboratory show that the F -statistical value of the damage state compared with the initial state is an effective indicator of the damage extent of the structure, and the F -statistical value of two adjacent states is also effective to monitor any abnormal change in the structure without an intact database. From the energy distribution of the response obtained at mid-span of the reinforced concrete beam in the laboratory, the F -statistical value (mean) is found robust to detect both local and global damage close to mid-span, while those of the higher order statistics are more robust to detect local damage at different locations of the structure. It is believed that the combine use of all four indicators from energy distribution at selected frequency range could monitor the extent and location of local damages in a structure.

Acknowledgements

The work described in this paper was supported by a grant from the Hong Kong Research

Grant Council Project No. Poly U 5043/02E and a grant from the Hong Kong Polytechnic University Research Funding Project No. G-YW98.

References

- Bagheri, A., Ghodrati A.G., Khorasani, M. and Bakhshi, H. (2011), "Structural damage identification of plates based on modal data using 2D discrete wavelet transform", *Struct. Eng. Mech.*, **40**(1), 13-28.
- Beheshti-Aval, S.B., Taherinasab, M. and Noori, M. (2011), "Using harmonic class loading for damage identification of plates by wavelet transformation approach", *Smart Structures and Systems*, **8**(3), 253-274.
- Berry, D.A. and Lindgren, B.W. (1996), *Statistics: Theory and Methods*, Duxbury Press, CA, USA.
- Carden, E.P. and Fanning, P. (2004) "Vibration based condition monitoring: A review", *Struct. Health Monit.*, **3**(4), 355-377.
- Coifman, R.R., Meyer, Y. and Wickerhauser, M.V. (1992), "Wavelet analysis and signal processing", *Wavelets and Their Application*, 153-178, Jones and Bartlett, Boston, MA.
- Davison, A.C. and Hinkley, D.V. (1997), *Bootstrap methods and their application*, Cambridge University Press, U.K.
- Doebling, S.W., Farrar, C.R. and Prime, M.B. (1998), "A summary review of vibration-based damage identification methods", *Shock Vib. Digest*, **30**(2), 91-105.
- Fang, S.E. and Perera, R. (2009), "A response surface methodology based damage identification technique", *Smart Mater. Struct.*, **18**(6), 1-14.
- Farrar, C.R., Doebling, S.W. and Nix, D.A. (2001), "Vibration-based structural damage identification", *Philos. T. R. Soc. A*, **359**(1778), 131-149.
- Glantz, S.A. (2002), *Primer of Biostatistics*, Fifth Edition, McGraw-Hill Professional.
- Gokdag, H. (2011), "Wavelet-based damage detection method for a beam-type structure carrying moving mass", *Struct. Eng. Mech.*, **38**(1), 81-97.
- Gul, M. and Catbas, F.N. (2009), "Statistical pattern recognition for structural health monitoring using time series modelling: theory and experimental verifications", *Mech. Syst. Signal Pr.*, **23**(7), 2192-2204.
- Hou, Z., Noori, M. and St. Amand, R. (2000), "Wavelet-based approach for structural damage detection", *J. Eng. Mech. ASCE*, **126**(7), 677-683.
- Iwasaki, A., Todoroki, A., Shimamura, Y. and Kobayashi, H. (2004), "An unsupervised statistical damage detection method for structural health monitoring", *Smart Mater. Struct.*, **13**(5), 80-85.
- Iwasaki, A., Todoroki, A., Sugiya, T., Izumi, S. and Sakai, S. (2005), "Unsupervised statistical damage diagnosis for structural health monitoring of existing civil structures", *Smart Mater. Struct.*, **14**(3), 154-161.
- Law, S.S., Ward, H.S., Shi, G.B., Chen, R.Z., Waldron, P. and Taylor, C. (1995), "Dynamic assessment of bridge load carrying capacities – I", *J. Struct. Eng.-ASCE*, **121**(3), 478-487.
- Law, S.S., Li, X.Y., Zhu, X.Q. and Chan, S.L. (2005) "Structural damage detection from wavelet packet sensitivity", *Eng. Struct.*, **27**(9), 1339-1348.
- Li, X.Y. and Law, S.S. (2008), "Condition assessment of structures under ambient white noise excitation", *AIAA J.*, **46**(6), 1395-1404.
- Mallat, S. (1999), *A Wavelet Tour of Signal Processing*, Academic Press.
- Markou, M. and Singh, S. (2003), "Novelty detection: a review—part 1: statistical approaches", *Signal Process.*, **83**(12), 2481-2497.
- Miller, I. and Miller, M. (2004), *JOHN E. Freund's Mathematical Statistics: with applications*, 7th Edition, Pearson/Prentice Hall, Upper Saddle River, New Jersey.
- Ren, W.X. and Sun, Z.S. (2008), "Structural damage identification by using wavelet entropy", *Eng. Struct.*, **30**(10), 2840-2849.
- Ruotolo, R. and Surace, C. (1997), "A statistical approach to damage detection through vibration

- monitoring”, *Proceedings of the 5th Pan American Congress of Applied Mechanics*, Puerto, Rice.
- Snedecor, G.W. and Cochran, W.G. (1989), *Statistical methods*, 8th Edition, Ames: The Iowa State University Press.
- Sohn, H., Czarnecki, J.A. and Farrar, C.R. (2000), “Structural health monitoring using statistical process control”, *J. Struct. Eng.-ASCE*, **126**(11), 1356-1363.
- Sohn, H. and Farrar, C.R. (2001), “Damage diagnosis using time series analysis of vibration signals”, *Smart Mater. Struct.*, **10**(3), 446-451.
- Sohn, H., Farrar, C.R., Hemez, F.M., Shunk, D.D., Stinemates, D.W. and Nadler, B.R. (2003), *A Review of Structural Health Monitoring Literature: 1996-2001*, Los Alamos National Laboratory Report.
- Sohn, H. (2007), “Effects of environmental and operational variability on structural health monitoring”, *Philos. T. R. Soc. A*, **365**(1851), 539-560.
- Sun, Z. and Chang, C.C. (2002), “Structural damage assessment based on wavelet packet transform”, *J. Struct. Eng.- ASCE*, **128**(10), 1354-1361.
- Sun, Z. and Chang, C.C. (2004), “Statistical wavelet-based method for structural health monitoring”, *J. Struct. Eng.- ASCE*, **130**(7), 1055-1062.
- Worden, K., Manson, G. and Fieller, N.R.J. (2000), “Damage detection using outlier analysis”, *J Sound Vib*, **229**(3), 647-667.
- Yam, L.H., Yan, Y.J. and Jiang, J.S. (2003), “Vibration-based damage detection for composite structures using wavelet transform and neural network identification”, *Compos. Struct.*, **60**(4), 403-412.
- Yun, G.J., Lee, S.G., Carletta, J. and Nagayama, T. (2011), “Decentralized damage identification using wavelet signal analysis embedded on wireless smart sensors”, *Eng. Struct.*, **33**(7), 2162-2172.
- Zhang, J., Xu, Y.L., Xia, Y. and Li, J. (2008), “A new statistical moment-based structural damage detection method”, *Struct. Eng. Mech.*, **30**(4), 445-466.